Deformed band structures in neutron-rich $^{152–158}$Pm isotopes

S. Bhattacharyya,[1,2,*] E. H. Wang,[3] A. Navin,[4] M. Rejmund,[4] J. H. Hamilton,[3] A. V. Ramayya,[3] J. K. Hwang,[3] A. Lemasson,[4] A. V. Afanasjev,[5] Soumik Bhattacharya,[1,2] J. Ranger,[3] M. Caamaño,[6] E. Clément,[4] O. Delaune,[4] F. Farget,[4] G. de France,[4] B. Jacquot,[4] Y. X. Luo,[3,7] Yu. Ts. Oganessian,[8] J. O. Rasmussen,[7] G. M. Ter-Akopian,[8] and S. J. Zhu[9]

[1]*Variable Energy Cyclotron Centre, 1/AF Bidhannagar, Kolkata 700064, India*
[2]*Homi Bhabha National Institute, Training School Complex, Anushaktinagar, Mumbai-400094, India*
[3]*Department of Physics and Astronomy, Vanderbilt University, Nashville, Tennessee 37235, USA*
[4]*GANIL, CEA/DRF-CNRS/IN2P3, Boulevard Henri Becquerel, BP 55027, F-14076 Caen Cedex 5, France*
[5]*Department of Physics and Astronomy, Mississippi State University, Mississippi 39762, USA*
[6]*USC, Universidad de Santiago de Compostela, E-15706 Santiago de Compostela, Spain*
[7]*Lawrence Berkeley National Laboratory, Berkeley, California 94720, USA*
[8]*Joint Institute for Nuclear Research, RU-141980 Dubna, Russian Federation*
[9]*Department of Physics, Tsinghua University, Beijing 100084, People's Republic of China*

(Received 24 October 2017; revised manuscript received 3 August 2018; published 17 October 2018)

High spin band structures of neutron-rich $^{152–158}$Pm isotopes have been obtained from the measurement of prompt γ rays of isotopically identified fragments produced in fission of ^{238}U + ^{9}Be and detected using the VAMOS++ magnetic spectrometer and EXOGAM segmented Clover array at GANIL and also from the high statistics γ-γ-γ and γ-γ-γ-γ data from the spontaneous fission of ^{252}Cf using Gammasphere. The excited states in ^{157}Pm and those above the isomers in even-A Pm isotopes ^{152,154,156,158}Pm have been identified for the first time. The spectroscopic information on the rotational band structures in odd-A Pm isotopes has been extended considerably to higher spins and the possibility of the presence of reflection asymmetric shapes is explored. The configuration assignments are based on the results of cranked relativistic Hartree-Bogoliubov calculations. From the systematics of bands in odd-A Pm isotopes and weak population of opposite parity bands, octupole deformed shapes in neutron-rich Pm isotopes beyond $N = 90$ seem unlikely to be present.

DOI: 10.1103/PhysRevC.98.044316

I. INTRODUCTION

The many-body correlations in atomic nuclei can lead to various shapes other than those that are spherically symmetric. These include reflection symmetric prolate or oblate shapes having quadrupole deformation, triaxial shapes having both quadrupole deformation and axial asymmetry, and reflection asymmetric pear shape with static octupole deformation. The nuclei of the rare-earth region with $N = 88 - 90$ are well known to have transitional character: from nearly spherical or weakly deformed shapes for $N < 88$ to well-deformed shapes for $N > 90$. A deformed region beyond $N = 90$ is known from the systematics of the first excited states of even-even nuclei around $Z = 55$–66 [1]. The nuclei in the $A = 140$–150 mass region are expected to have octupole collectivity. This is because their Fermi levels lie between the $f_{7/2}$ and $i_{13/2}$ neutron orbitals and between the $d_{5/2}$ and $h_{11/2}$ proton orbitals, which differ by $\Delta j = \Delta l = 3$; this leads to an increase of octupole correlations [2,3]. The first experimental signature of octupole collectivity in this region was reported for neutron-rich Ba isotopes [4,5] and later on more definitively established in neutron-rich odd- and even-A Ba and Ce nuclei [6–9] and other rare-earth nuclei [10]. Direct evidence of static octupole deformation in neutron-rich nucleus ^{144}Ba has been reported recently [11].

There are several experimental fingerprints of static octupole deformation in nuclei, which are discussed in detail in Refs. [2,3,12]. One of them is the presence of specific features of rotational bands. Alternating parity bands with positive and negative parity states forming the sequence $I^+, (I+1)^-, (I+2)^+, \ldots$ appear in even-even nuclei [3]. Parity doublet bands are formed in odd and odd-odd nuclei. In these bands, parity doubling leads to the appearance of the pair of the states with spin I but opposite parities [3]. Note that a parity doublet band can be represented as a pair of alternating parity bands with simplexes $s = +i$ and $s = -i$ [3]. The opposite parity states of given simplex in parity doublet bands are typically connected by strong $E1$ transitions, which is another possible experimental signature of reflection asymmetric shape. However, the electric dipole moment is built from delicate balance of proton and neutron contributions [13]. As a result, low $B(E1)$ rates do not necessarily exclude static octupole deformation and vice versa. For example, the large $B(E1)$ strengths in $N = 92$ isotones ^{155}Eu and ^{157}Tb could also be explained without considering static octupole deformation [14]. The behavior of alternating-parity and parity doublet bands with spin offers another clue on the presence of static octupole deformation since the rotation could stabilize the octupole deformation

*Corresponding author: sarmi@vecc.gov.in

[13,15,16]. Therefore, to understand the evolution of nuclear shape and nature of deformation of nuclei in this region, it is important to have more experimental data on high spin states with increasing neutron number.

The observation of the bands with features typical for parity doublet bands in odd-A and odd-odd nuclei in this region has also lead to various theoretical efforts to interpret these results in terms of static octupole deformation [12,17]. Shell correction methods based on reflection asymmetric Woods-Saxon model were also used to explain the experimental observation of local quenching in $E1$ strength in some of the cases [13].

The heavier isotopes of rare-earth region, which are mostly neutron rich, can be accessed by the fission process. The spectroscopy of heavy fission fragments provides the opportunity to investigate deformation effects as a function of neutron number for a particular isotope chain. Pm nuclei, with a wide isotopic range, are good candidates to explore the evolution of deformation with neutron number and possible role of octupole deformation in this region. It may be noted that there are no stable isotopes of Pm and that the isotopes beyond ^{151}Pm are known only through radioactive decay studies [18–23], proton transfer measurements [24,25] and spontaneous fission of ^{252}Cf source [26]. This is mainly due to nonavailability of a suitable target-projectile combination to produce the nuclei in fusion evaporation reaction with large cross section. The high spin states of neutron-rich nuclei in this mass region can be efficiently produced in fission. Isotopic identification of nuclei is critical to carry out spectroscopy of these exotic nuclei. Usually the technique of high-fold γ-γ coincidences and the cross coincidence relationships among the heavy and light fragment partners of the fission process are utilized to assign the γ rays to a particular isotope. But in the case of extreme neutron-rich isotopes, for which not a single γ transition is known, it is very difficult to assign the γ rays to the level scheme of a particular isotope on the basis of only γ-γ coincidence. Furthermore, the presence of low-lying long-lived isomers in certain nuclei hinders the prompt coincidence between γ rays below and above the isomer. In such cases, even if some of the transitions below the isomer are known, the band structure above the isomer cannot be obtained by using high-fold γ coincidence techniques. Thus, a direct isotopic (A, Z) identification of nuclei is essential for an unambiguous assignment of γ rays. The high spin experimental data on neutron-rich Pm isotopes was very limited prior to this study. In fact, no in-beam high spin spectroscopic measurements are available beyond ^{151}Pm.

The bands with features typical for parity doublet bands extending to high spins have been found in odd-A Pm isotopes for $N = 86$ ^{147}Pm [27], $N = 88$ ^{149}Pm [28], and $N = 90$ ^{151}Pm [29,30]. The possibility of the presence of a reflection asymmetric shape at $N = 92$ has also been reported from the observation of enhanced $E1$ transitions between a couple of low-lying states of a band structure (which has typical features of parity doublet bands) in ^{153}Pm measured in β decay [20]. Although the band structures observed in ^{151}Pm and ^{153}Pm are very similar, the origin of the ground-state band in these two nuclei are quite different. In ^{151}Pm the band head of the ground band is $5/2^+$ based on the $[413]5/2^+$ configuration, originating from the $g_{7/2}$ orbital, whereas, the ground band in ^{153}Pm with larger prolate deformation is based on the configuration $[523]5/2^-$, originating from the high-j $h_{11/2}$ orbital. The rotational band based on the $\pi 5/2[532]$ state has also been identified in ^{155}Pm from the spontaneous fission of ^{252}Cf source [26], whereas no excited states in ^{157}Pm are reported so far. Recently, μs isomers are observed in ^{158,159,161}Pm, produced by in-flight fission of ^{238}U beam [31]. Few lower spin members of the rotational band in ^{159,161}Pm have also been observed in this study of delayed γ-ray spectroscopy of μs isomers. It would be interesting to extend the level structure of neutron-rich Pm isotopes to higher spins to understand the deformation effects as a function of N/Z and explore which kind of nuclear shapes (reflection symmetric quadrupole deformed or reflection asymmetric octupole deformed) exist at higher N/Z ratios.

For the neutron-rich odd-odd Pm isotopes, the information about the excited states is rather scarce, mainly because of the presence of long-lived low-lying isomers. Even the excitation energies of the long-lived isomers are not well determined in most of the cases. The spectroscopic information on the odd-odd neutron-rich Pm isotopes above $N = 90$ are reported from β decay or decay of isomeric transition studies [18,19,21–23,32]. Thus, the information about the structure of the states above the long-lived isomers of these odd-odd Pm isotopes can only be obtained by directly populating the high spin states via in-beam prompt spectroscopy. In the presence of a long-lived isomer, even if some of the γ rays below the high spin isomer are known, the assignment of γ rays above the isomer of a particular isotope is challenging, as γ-γ coincidences across a long-lived isomeric state are difficult. A few low spin states in ^{152}Pm are known from β decay of ^{152}Nd [18,19] and the existence of two high spin isomers [7.5 min $(4^{\pm})$ and 18 min $(\geqslant 6^+)$] have also been identified from these studies. The excited states of ^{154}Pm have been identified from the β decay of ^{154}Nd [21,22] and the existence of two isomeric levels of 2.8 min and 1.8 min with probable spin assignment of $J \leqslant 3$ were reported in Ref. [32] from the observed β decay and associated log-ft values corresponding to the β decay of these isomeric states to ^{154}Sm. For ^{156}Pm, an isomeric state at 150.3 keV (with a tentative J^π of 1^-) was identified and found to deexcite to the ground state by a $M3$ transition [23]. In Ref. [26] the γ rays from the high spin states of ^{156}Pm were reported, but, as discussed later in this paper, those γ rays actually belong to ^{157}Pm. No spectroscopic information above these isomeric states in ^{152,154,156}Pm are known prior to the present work. In the case of ^{158}Pm, the evidence of the existence of a μs isomer and the isomeric transition decay from that state has recently been reported [31]. No other excited states of ^{158}Pm are known prior to the present study.

In the present work, the γ rays are detected with EXOGAM [33] segmented Clover detectors, in coincidence with the detected fission fragment at the focal plane of VAMOS++ spectrometer [34] with isotopic (A, Z) identification. Thus, the assignment of γ rays to a particular isotope is unambiguous. Once the identification of the γ ray is ensured, the details of the level scheme at higher spin can be obtained from the high-fold γ coincidence data from ^{252}Cf fission

using Gammasphere. In the present work the prompt γ rays of neutron-rich Pm isotopes have been reported up to $N = 97$ and the results are interpreted in terms of rotational band structures. The in-beam populations of the prompt transitions of ^{153}Pm is reported for the first time and the level scheme has been extended considerably to higher spins up to $(29/2^-)$. The rotational band of ^{155}Pm has also been extended to higher spins compared to previous work [26]. The transitions of ^{157}Pm are reported for the first time in this paper. Some of these transitions were assigned to ^{156}Pm in Ref. [26] from the measurement of spontaneous fission of ^{252}Cf. For the odd-odd Pm isotopes, the first in-beam prompt spectroscopy measurements of $^{152-158}$Pm are reported from the present work. The band structures above the high spin isomers in these nuclei have been identified for the first time. The results are discussed from the systematics of band properties. The cranked relativistic Hartree-Bogoliubov calculations are also performed to understand configuration assignments.

The paper is organized as follows. Section II describes the details of experiment and the analysis of experimental data. Obtained results and the level schemes for odd-A and even-A Pm nuclei are presented in Sec. III. The discussion of the observables of interest and the interpretation of the physical situation are carried out in Sec. IV. Finally, Sec. V summarizes the results of our work.

II. EXPERIMENT

The measurements were carried out by using two complementary methods, namely (i) by direct identification of the fission fragments (A, Z) at the focal plane of the large acceptance magnetic spectrometer VAMOS++ and detection of corresponding in-beam γ rays in coincidence and (ii) by detection of high-fold γ coincidence data from ^{252}Cf spontaneous fission. The first method improves the selectivity and sensitivity of the measurements by unambiguous identification of the particular isotopes and the second one facilitates the study of high spin level structure using high-fold γ coincidence techniques. The power of combining the two sets of data has been demonstrated earlier in case of study of neutron-rich Pr isotopes [35].

The measurements of (A, Z) identification of the fission fragments and fragment-γ coincidence were carried out at Grand Accelerateur National d'Ions Lourds (GANIL) using a ^{238}U beam at 6.2 MeV/u ($\sim$0.2 pnA) on a 10-μm thick ^{9}Be target. The fission fragments were directly identified by mass number (A), atomic number (Z) in the VAMOS++ magnetic spectrometer [34] placed at 20° with respect to the beam axis. The elemental identification (Z) of the fission fragments was obtained from energy loss (ΔE) in the ionization chamber and the total energy (E) measured by the Si detectors, placed at the focal plane of VAMOS++ spectrometer. The time of flight (TOF) was measured between the two Multi-Wire Parallel Plate Avalanche Counters (MWPPAC), one placed just after the target and another at the focal plane. The (x, y) positions of the detected fragments were determined by the two Drift chambers at the focal plane. The various measured positions, energies, and times along with the known magnetic field were used to determine, on an event-by-event basis, the mass (M),

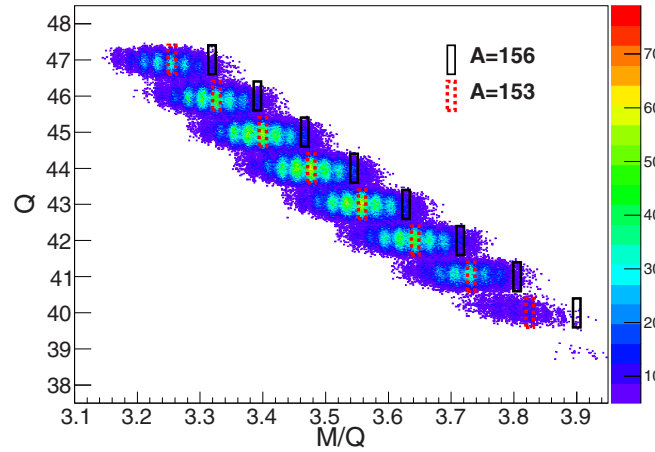

FIG. 1. Charge state (Q) as a function of the mass over charge (M/Q) after selection of Pm $(Z = 61)$ in the ^{238}U + ^{9}Be reaction at 6.2 MeV/u. The figure shows the identified Pm isotopes from various charge states at the focal plane of the VAMOS++ spectrometer. Identification of $A = 153$ (red, dash box) and $A = 156$ (black, solid box) from each charge state (Q) are labeled. The color scale represents the counts along the Z axis.

charge state (Q), Z, and the velocity vector $(\vec{v})$ for the detected fragment [34]. The magnetic rigidity $(B\rho)$ was obtained by applying a reconstruction procedure. The parameters (M/Q) and (M) were obtained independently using the reconstructed magnetic rigidity and from the measured velocity and total energy. A two-dimensional spectrum of Q and M/Q provides a clean and unambiguous identification of various isotopes detected at the focal plane. Figure 1 shows the identification plot of Q vs M/Q after selection of $Z = 61$. The prompt γ rays were measured in coincidence with the isotopically identified fragments, using the EXOGAM array [33], consisting of 11 Compton-suppressed segmented Clover HPGe detectors placed at 15 cm from the target position. The γ-ray energies of the fragments were obtained event by event after Doppler correction from the measured $\vec{v}$ using the VAMOS++ spectrometer and with the known angle of the segment of the relevant clover detector [34,36]. More details of the setup and the measurements at GANIL can be found in Refs. [37,38].

The high-fold γ coincidence data were obtained from the measurements of ^{252}Cf spontaneous fission at the Lawrence Berkeley National Laboratory (LBNL) using 101 HPGe detectors of Gammasphere. A 62-μCi ^{252}Cf source was sandwiched between two Fe foils of thickness 10 mg/cm^2. The data were sorted into γ-γ-γ and higher-fold γ events to form three-dimensional (3D) cube and 4D cubes and were analyzed using the RADWARE package [39]. More details of this experiment and analysis procedures can be found in Refs. [40,41].

III. RESULTS

A. odd-A Pm isotopes

Doppler corrected γ-ray spectra of odd-A Pm isotopes, detected in the present work by EXOGAM segmented Clover detectors, after the (A, Z) selection of the respective isotopes

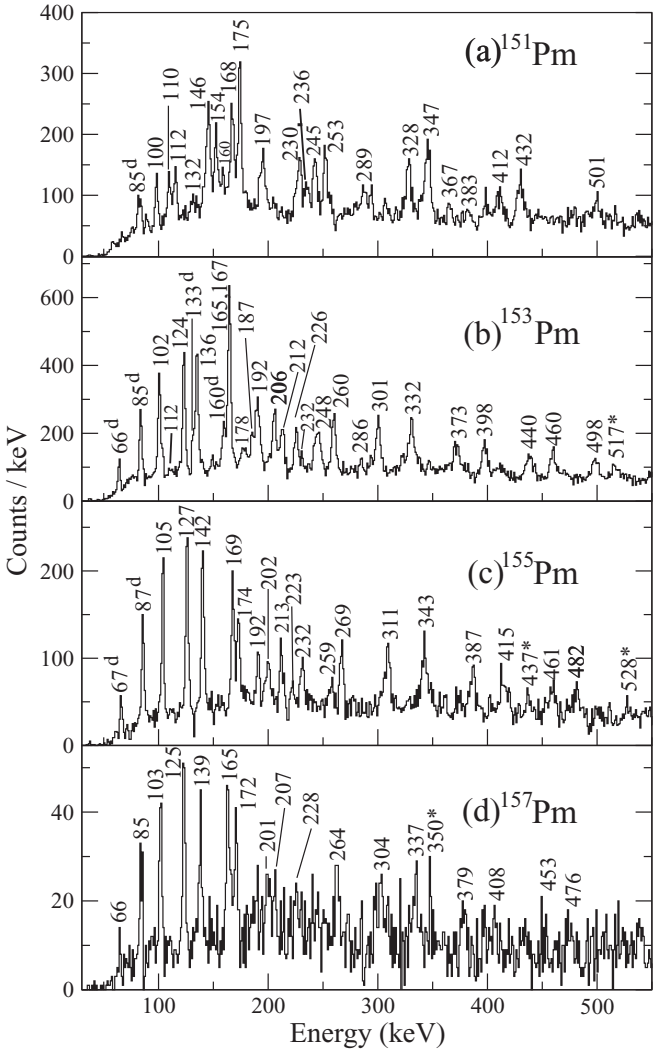

FIG. 2. (A, Z) gated Doppler corrected singles γ spectra of odd-A $^{151-157}$Pm, obtained from the fragment-γ coincidences in ^{238}U + ^{9}Be-induced fission data. The γ rays earlier observed from β decay are marked as "d". The γ rays marked as "*" are assigned to the respective odd-A Pm isotopes from the corresponding (A, Z) coincidence, but could not be placed in the level scheme.

at the focal plane of VAMOS++ spectrometer, are shown in Fig. 2. All the transitions of ^{151}Pm up to spin 27/2 $\hbar$, observed in the present work confirm those previously reported [29,30]. The corresponding spectrum is shown in Fig. 2(a) to highlight the quality of data. For neutron-rich odd-A Pm isotopes, transitions known from previous β-decay studies, are labeled. Some of the γ rays (as shown in Fig. 2), though identified as belonging to the corresponding odd-A Pm isotopes through (A, Z) gating, could not be placed in the respective level schemes due to insufficient γ-γ coincidence information. The γ rays of ^{153,157}Pm from in-beam prompt spectroscopy are being reported for the first time here and new level schemes are proposed. New transitions in ^{155}Pm have also been identified and the level scheme has been extended to higher spins compared to that previously reported [26]. The γ rays, assigned to various odd-A Pm isotopes, along with their

TABLE I. The energies (E_γ) and relative intensities (I_γ) of the γ rays assigned to different odd-A Pm isotopes along with the spin and parity of the initial (J_i^π) and the final (J_f^π) states and the energy of the initial state (E_i).

E_γ (keV)[a]	E_i (keV)[b]	J_i^π	→	J_f^π	I_γ[c](Err.)
^{153}Pm					
66	66	$7/2^-$	→	$5/2^-$	24(6)
85	151	$9/2^-$	→	$7/2^-$	41(11)
102	253	$(11/2^-)$	→	$9/2^-$	74(12)
112	311	$(11/2^+)$	→	$(9/2^+)$	9(5)
124	376	$(13/2^-)$	→	$(11/2^-)$	100(9)
133	199	$(9/2^+)$	→	$7/2^-$	33(6)
136	512	$(15/2^-)$	→	$(13/2^-)$	98(8)
151	151	$9/2^-$	→	$5/2^-$	15(8)
160	311	$(11/2^+)$	→	$9/2^-$	36(8)
165	678	$(17/2^-)$	→	$(15/2^-)$	158(9)[d]
167	845	$(19/2^-)$	→	$(17/2^-)$	-[d]
178	430	$(13/2^+)$	→	$(11/2^-)$	20(6)
187	253	$(11/2^-)$	→	$7/2^-$	30(6)
192	1243	$(23/2^-)$	→	$(21/2^-)$	80(6)
206	1051	$(21/2^-)$	→	$(19/2^-)$	71(8)
212	1703	$(27/2^-)$	→	$(25/2^-)$	59(6)
226	376	$(13/2^-)$	→	$9/2^-$	48(11)
232	430	$(13/2^+)$	→	$(9/2^+)$	14(5)
248	1491	$(25/2^-)$	→	$(23/2^-)$	45(8)
260	512	$(15/2^-)$	→	$(11/2^-)$	76(9)
286	1989	$(29/2^-)$	→	$(27/2^-)$	12(3)
301	678	$(17/2^-)$	→	$(13/2^-)$	92(8)
332	845	$(19/2^-)$	→	$(15/2^-)$	98(9)
373	1051	$(21/2^-)$	→	$(17/2^-)$	56(8)
398	1243	$(23/2^-)$	→	$(19/2^-)$	79(11)
440	1491	$(25/2^-)$	→	$(21/2^-)$	76(12)
460	1703	$(27/2^-)$	→	$(23/2^-)$	79(9)
498	1989	$(29/2^-)$	→	$(25/2^-)$	68(12)
^{155}Pm					
67	67	$(7/2^-)$	→	$5/2^-$	27 (8)
87	154	$(9/2^-)$	→	$(7/2^-)$	54 (14)
105	259	$(11/2^-)$	→	$(9/2^-)$	73 (5)
127	386	$(13/2^-)$	→	$(11/2^-)$	100 (5)
142	528	$(15/2^-)$	→	$(13/2^-)$	92 (5)
169	698	$(17/2^-)$	→	$(15/2^-)$	81 (5)
174	872	$(19/2^-)$	→	$(17/2^-)$	62 (5)
192	259	$(11/2^-)$	→	$(7/2^-)$	27 (5)
202	1286	$(23/2^-)$	→	$(21/2^-)$	24 (5)
213	1084	$(21/2^-)$	→	$(19/2^-)$	41 (5)
223	1769	$(27/2^-)$	→	$(25/2^-)$	27 (5)
232	387	$(13/2^-)$	→	$(9/2^-)$	46 (5)
259	1546	$(25/2^-)$	→	$(23/2^-)$	14 (3)
269	528	$(15/2^-)$	→	$(11/2^-)$	51 (5)
311	698	$(17/2^-)$	→	$(13/2^-)$	78 (8)
343	872	$(19/2^-)$	→	$(15/2^-)$	70 (8)
387	1084	$(21/2^-)$	→	$(17/2^-)$	46 (5)
415	1286	$(23/2^-)$	→	$(19/2^-)$	38 (5)
461	1546	$(25/2^-)$	→	$(21/2^-)$	38 (5)
482	1769	$(27/2^-)$	→	$(23/2^-)$	41 (5)
^{157}Pm					
66	66	$(7/2^-)$	→	$(5/2^-)$	2(1)
85	151	$(9/2^-)$	→	$(7/2^-)$	5(2)
103	254	$(11/2^-)$	→	$(9/2^-)$	6(1)

TABLE I. *(Continued.)*

E_γ (keV)[a]	E_i (keV)[b]	J_i^π	→	J_f^π	I_γ[c](Err.)
^{153}Pm					
125	379	$(13/2^-)$	→	$(11/2^-)$	9(1)
139	518	$(15/2^-)$	→	$(13/2^-)$	6(2)
151	151	$(9/2^-)$	→	$(5/2^-)$	-[e]
165	683	$(17/2^-)$	→	$(15/2^-)$	10(1)
172	855	$(19/2^-)$	→	$(17/2^-)$	6(1)
188	254	$(11/2^-)$	→	$(7/2^-)$	2(1)
201	1263	$(23/2^-)$	→	$(21/2^-)$	4(1)
207	1062	$(21/2^-)$	→	$(19/2^-)$	4(1)
228	379	$(13/2^-)$	→	$(9/2^-)$	2(1)
252	1515	$(25/2^-)$	→	$(23/2^-)$	2(1)
264	518	$(15/2^-)$	→	$(11/2^-)$	7(2)
304	683	$(17/2^-)$	→	$(13/2^-)$	6(1)
337	855	$(19/2^-)$	→	$(15/2^-)$	6(1)
379	1062	$(21/2^-)$	→	$(17/2^-)$	2(1)
408	1263	$(23/2^-)$	→	$(19/2^-)$	3(1)
453	1515	$(25/2^-)$	→	$(21/2^-)$	4(2)
476	1739	$(27/2^-)$	→	$(23/2^-)$	7(4)

[a]γ-ray energy uncertainties are typically $\pm$ 0.2 keV, $\pm$ 0.5 keV and $\pm$ 1 keV around 200 keV, 500 keV, and 1 MeV, respectively.
[b]The maximum uncertainty of the level energy is up to 0.5%.
[c]Intensities are normalized to 100 for ^{153,155}Pm and to 10 for ^{157}Pm. The errors quoted are the fitting errors.
[d]Combined intensity of 165 and 167 keV.
[e]Weak transition, intensity could not be determined.

relative intensities and the level energies, obtained from the (A, Z) gated spectra are shown in Table I. The quoted errors are the fitting errors. The probable spin-parity assignments of the initial and final states of the transitions have been obtained using the known systematics of odd-A Pm isotopes. The statistics were not enough to carry out any angular distribution or polarization measurements for such neutron-rich nuclei.

Information on the excited states of ^{153}Pm was known from (t, α) and $(d, ^3\text{He})$ transfer reactions [24,25]. The levels pertaining to the bands based on Nilsson orbitals $5/2^-[532]$, $5/2^+[413]$, $3/2^+[411]$ were identified from the measured particle angular distributions, without detection of any decaying γ transitions between the states. The first indication of band structure in ^{153}Pm, which has typical features of parity doublet bands, was reported from β-decay measurements [20]. In the present work the first information on the high spin states in ^{153}Pm is obtained, which is extended up to 1989 keV $(29/2^-)$ from in-beam prompt γ spectroscopy measurements. The γ spectrum in coincidence with the ^{153}Pm fragments identified using the VAMOS++ spectrometer is shown in Fig. 2(b). The γ spectra corresponding to the gates of 102, 136, and 165 keV transitions are shown in Fig. 3, obtained from the γ-γ matrix after selection of ^{153}Pm fragment from $^{238}\text{U} + ^9\text{Be}$-induced fission data. The mutual coincidence of 102, 124, 136, 165, 167 keV γ rays can be clearly seen from the coincidence spectra shown in Figs. 3(a)–3(c). The presence of doublet 165–167 keV could be confirmed from the γ-γ coincidence, as it is evident from Fig. 3(c) corresponding to the coincidence spectrum of 165 keV transition. The presence of other transitions decaying from higher excited states of ^{153}Pm, is also visible from the coincidence spectra of Figs. 3(a)–3(c). The triple coincidence spectra by gating on the 39 keV Pm x rays and other strong transitions of 102, 124, and 136 keV are shown in Fig. 4. The presence of cascade γ rays in the $5/2^-$ ground band of ^{153}Pm is clearly visible from these spectra. The level scheme of ^{153}Pm, as shown in Fig. 5, has been obtained on the basis of energy systematics of known odd-A Pm isotopes, the γ-γ coincidence measurements, and intensity balance. The placement of the crossover transitions are also made from the energy-sum systematics. The spin parity of the $7/2^-$, $9/2^-$ states are adopted from a previous work on β decay [20]. In the present work, the data statistics for each detector angle was insufficient to carry out an angular distribution analysis. Therefore, the spin parities of the other excited levels are only tentatively assigned from the systematics of odd-A Pm isotopes. The observed intensities of transitions placed in the level scheme of ^{153}Pm and the corresponding excited levels

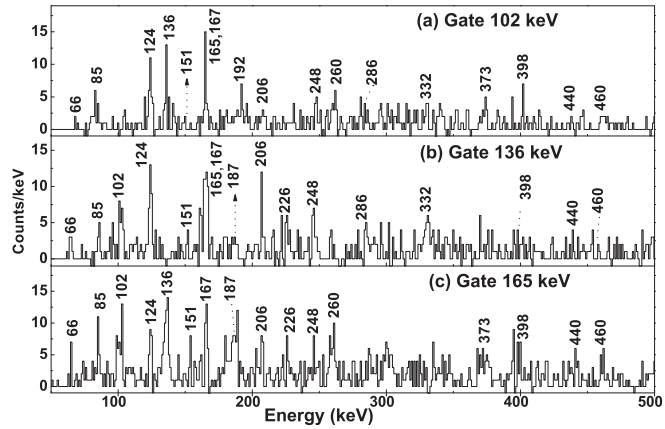

FIG. 3. Coincidence spectra corresponding to the gates on the (a) 102, (b) 136, and (c) 165 keV transitions in ^{153}Pm, obtained from the $^{238}\text{U} + ^9\text{Be}$-induced fission data.

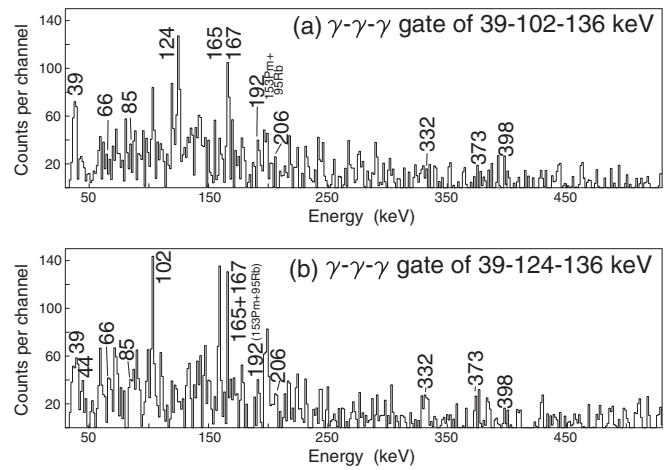

FIG. 4. Coincidence spectra corresponding to triple gates of the transitions in ^{153}Pm, obtained from the ^{252}Cf spontaneous fission data. (a) 39 (Pm x ray)-102-136 keV coincidence spectrum and (b) 39 (Pm x ray)-124-136 keV coincidence spectrum.

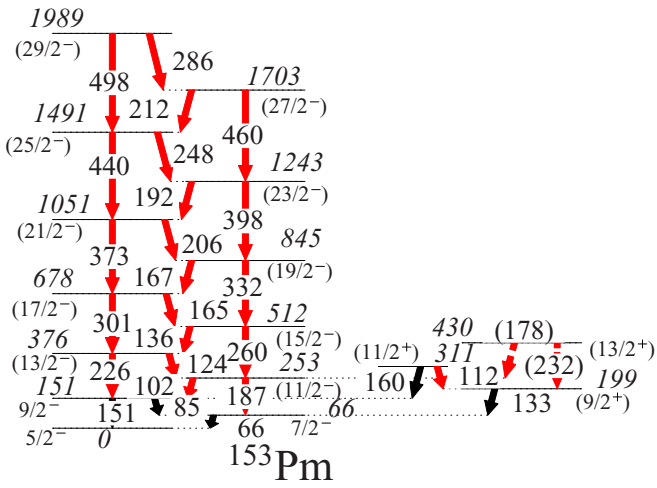

FIG. 5. The level scheme of ^{153}Pm proposed in the present work. The new transitions placed from the present work are shown in red and the previously known transitions from β decay are shown in black. The spin parity of the levels are tentatively assigned from the systematics of odd-A Pm isotopes, except for $7/2^-$ and $9/2^-$ levels, which are adopted from Ref. [20].

with tentative spin-parity assignments are given in Table I. It may be noted that the low-energy dipole transitions can be significantly converted and contain a mixing of higher-order multipoles. As mixing ratios (from angular distributions) of the transitions or the conversion electrons could not be measured in the present experiment, therefore, only the observed γ-ray intensities are shown in Table I. The intensity mismatch for some of the lower-lying states ($7/2^-$, $9/2^-$, and $11/2^-$) can be due to the fact that the low-energy dipole transitions are not pure and depending on the mixing ratios the conversion coefficients will be altered.

The presence of a parity doublet band in ^{153}Pm was indicated earlier in Ref. [20]. The transitions pertaining to this band, as reported in Ref. [20], could also be confirmed from the present data. From the present measurement, the 112 keV γ ray has been placed in this band as the transition from $(11/2^+)$ to $(9/2^+)$ level. Also, the 178 keV and 232 keV γ rays have been tentatively placed in this band, as these two transitions could not be observed in coincidence with any of the strong transitions of the band based on the $(5/2^-)$ state. Though γ-γ coincidence information could not be obtained for these transitions due to limited statistics, their presence in ^{153}Pm is confirmed, as the γ spectra in the present work have been obtained after (A, Z) identification.

The spectroscopic information on the excited states of ^{155}Pm and the associated γ rays were first known from the study of the β decay of ^{155}Nd [42]. Later, the existence of a rotational band extending up to $(23/2^-)$ in ^{155}Pm was reported [26] from the measurements of ^{252}Cf fission. This band has been extended up to $(27/2^-)$ in the present measurements. The γ-ray singles spectrum, as obtained using EXOGAM Clover array, in coincidence with detected ^{155}Pm at the focal plane of VAMOS++ spectrometer is shown in Fig. 2(c). The new transitions as compared to earlier reported [26] are

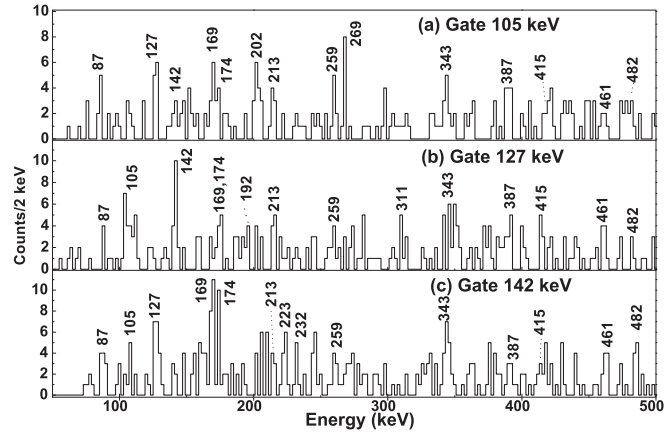

FIG. 6. Coincidence spectra corresponding to the gates on the (a) 105, (b) 127, and (c) 142 keV transitions in ^{155}Pm, obtained from the ^{238}U + ^{9}Be-induced fission data.

observed from this spectrum. The γ spectra corresponding to the gates of 105, 127, and 142 keV transitions are shown in Fig. 6, obtained from the γ-γ matrix after selection of ^{155}Pm fragment from ^{238}U + ^{9}Be-induced fission data. The placement of 105, 127, and 142 keV γ rays in coincidence with each other and the higher-lying transitions are supported from the coincidence spectra shown in Figs. 6(a)–6(c). Coincidence of the transitions are checked using various gating conditions and also from different added gates. A coincidence spectrum corresponding to double gates of 39 keV (Pm x ray) and 127 keV, obtained from ^{252}Cf data, is shown in Fig. 7. In this coincidence spectrum, the 159 and 217 keV peaks appear due to the presence of 126-159-218-217 cascade in ^{103}Nb and its partner La K_β x ray at 38 keV, which is present as a contamination in ^{155}Pm. The 217 peak could also come from ^{94}Rb fission partner in this case. The energy sum, intensities and the coincidence information of the observed γ rays are used to obtain the level scheme, as shown in Fig. 8. The spin parities indicated in Fig. 8 are only tentative, as angular distribution and polarization measurements were not possible from the present data. Also, it may be noted that no indication of any side band could be found for ^{155}Pm from the present data.

The excited states of ^{157}Pm are identified for the first time from the present measurements. Some of the transitions were earlier assigned to ^{156}Pm [26]. The incorrect placement was mainly due to problem of identification only from the

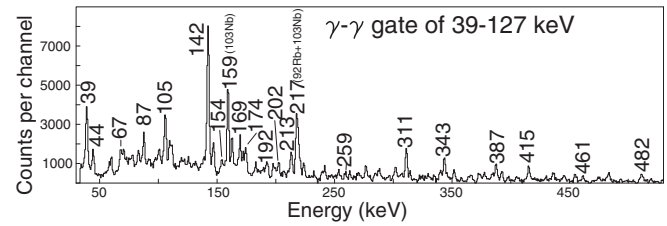

FIG. 7. Coincidence spectrum corresponding to the double gates of 39 (Pm x ray)-127 keV transitions in ^{155}Pm, obtained from the ^{252}Cf spontaneous fission data.

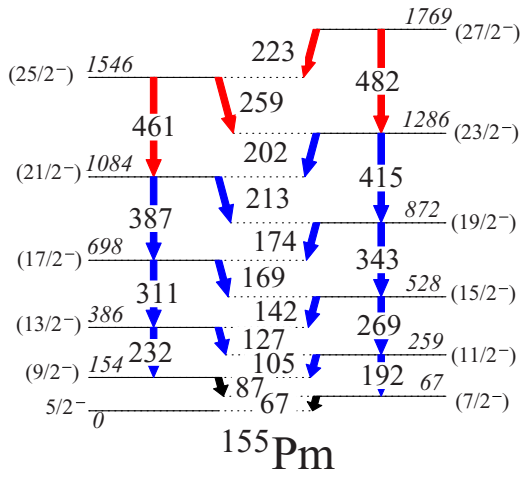

FIG. 8. Level scheme of ^{155}Pm proposed in the present work. The new transitions obtained in the present work are shown in red. The transitions previously known from β decay and ^{252}Cf fission are shown in black and blue, respectively. The spin parity of the levels shown are tentatively assigned from the systematics of odd-A Pm isotopes.

high-fold γ coincidence data for such exotic nuclei with a small production cross section. In the present work, the particular fragment is directly isotopically identified using the VAMOS++ spectrometer and the corresponding Doppler corrected γ rays are detected by EXOGAM segmented Clover array, leading to an unambiguous identification of the relevant transitions. The γ-ray singles spectrum in coincidence with detected ^{157}Pm fragments is shown in Fig. 2(d). The γ-γ coincidences for such neutron-rich nucleus were not possible from the measurements of ^{238}U + ^{9}Be reaction, but were obtained from ^{252}Cf fission data of Gammasphere array. The two representative coincidence spectra corresponding to double gates of 39 keV (Pm x ray) and 264 keV, 39 keV (Pm x ray), and 103 keV are shown in Fig. 9. The proposed level scheme

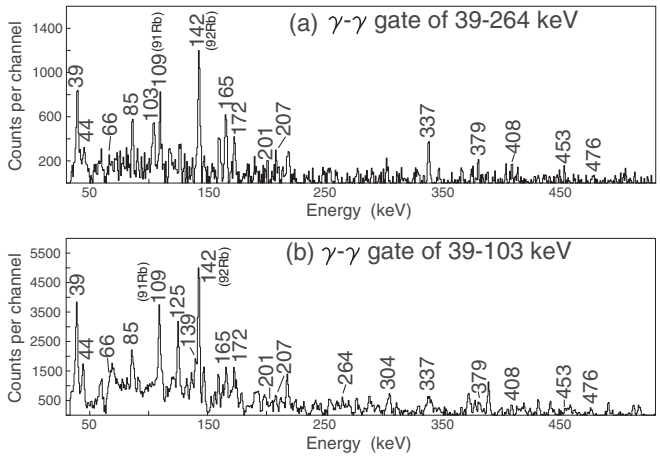

FIG. 9. Coincidence spectra corresponding to the double gates of the transitions in ^{157}Pm, obtained from the ^{252}Cf spontaneous fission data. (a) 39 (Pm x ray)-264 keV coincidence spectrum and (b) 39 (Pm x ray)-103 keV coincidence spectrum.

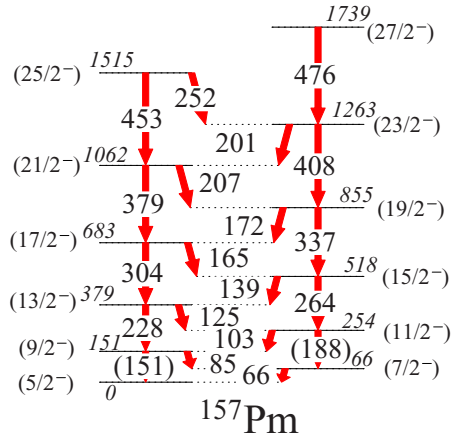

FIG. 10. Level scheme of ^{157}Pm proposed in the present work. All the new transitions in the scheme are from the present work and are shown in red. The spin parity of the levels shown are only tentative, assigned from the systematics of odd-A Pm isotopes.

of ^{157}Pm, obtained from the present work, is shown in Fig. 10. Only transitions seen in Fig. 2(d) and in multiple coincidence gates such as in Fig. 9, are placed in Fig. 10. An indication of the transitions 151 keV and 188 keV could be observed in (A, Z) gated spectra. These transitions are tentatively placed as the $E2$ crossover transitions corresponding to $(9/2^-)$ to $(5/2^-)$ and $(11/2^-)$ to $(7/2^-)$ states, respectively. The level scheme is obtained mainly from the energy level systematics of the neighboring isotopes, energy-sum, intensity balance, and coincidence information. For certain levels ($11/2^-$ state) the observed γ-ray intensities feeding in and decaying out of the level are imbalanced. This can be accounted for by considering the proper conversion of lower-energy dipole γ rays according to their mixing with higher-order multipoles. Spin parity of the states are only tentatively assigned from the systematics of odd-A Pm isotopes of lower masses.

B. Odd-odd Pm isotopes

For odd-odd Pm isotopes, the present work reports the first in-beam measurements of prompt γ rays of neutron-rich ^{152,154,156,158}Pm isotopes. The Doppler corrected γ-ray spectra of odd-odd Pm isotopes, detected in the present work in coincidence with the respective isotopes identified at the focal plane of VAMOS++ spectrometer are shown in Fig. 11. The γ rays, which could not be placed in the level schemes of respective even-A Pm isotopes due to lack of γ-γ coincidence information, are labeled in Fig. 11 (see caption of Fig. 11). However, the identification of these transitions to the corresponding even-A Pm isotopes are confirmed from (A, Z) gating condition. All these neutron-rich odd-odd Pm isotopes are known to have long-lived isomers and the information on excited states of these isotopes were extracted only from β decays. Prior to this study, the information on the high spin states of these neutron-rich nuclei were not available. This is because these states are difficult to populate in reactions other than fission and unambiguous assignment of the γ transitions of such neutron-rich nuclei cannot be made without direct

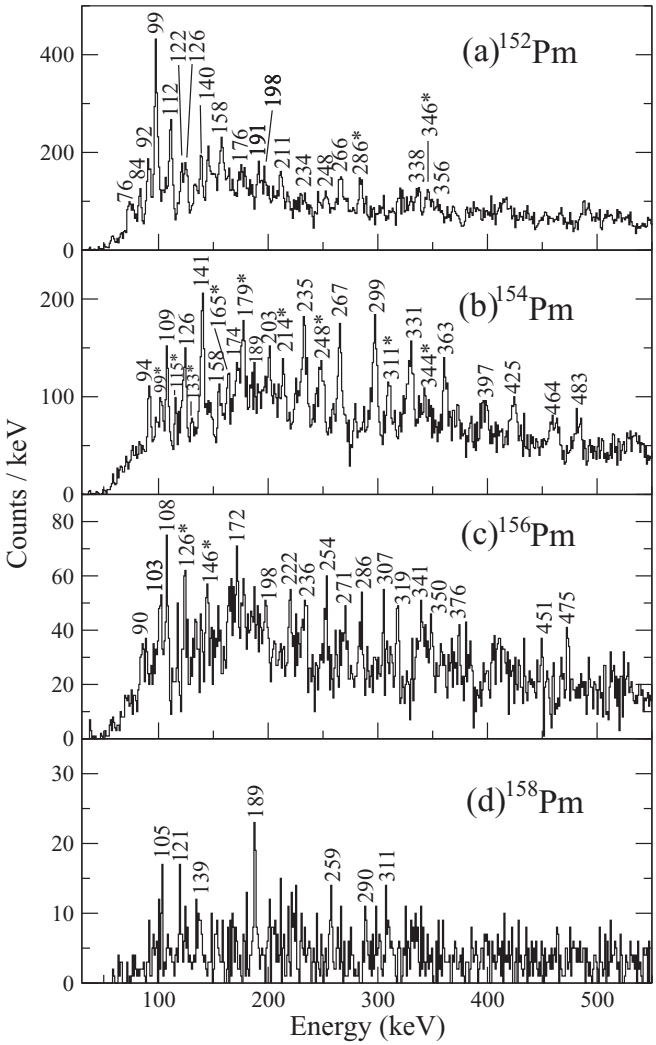

FIG. 11. (A, Z) gated Doppler corrected singles γ spectra of $^{152-158}$Pm, obtained from the fragment-γ coincidence in ^{238}U + ^{9}Be-induced fission data. The γ rays marked as "*" are assigned to the respective even-A Pm isotopes from the corresponding (A, Z) coincidence, but could not be placed in the level schemes.

identification of the corresponding isotope in coincidence. In particular, the presence of long-lived isomers make the situation more complicated, as correlation of the transitions below and above the isomer is not possible only from prompt γ-γ coincidence without any isotopic identification. In the present work, only the prompt in-beam γ rays are detected with isotopic identification as the experimental setup was not optimized to detect the delayed γ rays. The γ rays, assigned to various even-A Pm isotopes, along with their relative intensities, obtained from the (A, Z) gated spectra are shown in Table II. The probable spin parity the initial and final states are only tentatively assigned from the systematics of even-A Pm isotopes. The level energies given in Table II are with respect to a reference level and the quoted errors are the fitting errors. The γ rays observed and the proposed level schemes of particular cases are discussed below.

The precise measurement of the low spin levels of ^{152}Pm were established from the decay of mass separated ^{152}Nd [19].

TABLE II. The energies (E_γ) and relative intensities (I_γ) of the γ rays assigned to different even-A Pm isotopes along with the probable spin and parity of the initial (J_i^π) and the final (J_f^π) states and the energy of the initial state (E_i).

E_γ (keV)[a]	E_i (keV)[b]	J_i^π	→	J_f^π	I_γ[c](Err.)
^{152}Pm					
76	76	(I_0+1)	→	(I_0)	29 (8)
84	160	(I_0+2)	→	(I_0+1)	31 (8)
92	251	(I_0+3)	→	(I_0+2)	58 (13)
99	350	(I_0+4)	→	(I_0+3)	100 (15)
112	462	(I_0+5)	→	(I_0+4)	69 (6)
122	584	(I_0+6)	→	(I_0+5)	44 (6)
126	710	(I_0+7)	→	(I_0+6)	46 (6)
140	850	(I_0+8)	→	(I_0+7)	29 (4)
158	1206	(I_0+10)	→	(I_0+9)	19 (8)
160	160	(I_0+2)	→	(I_0)	54 (10)
176	251	(I_0+3)	→	(I_0+1)	25 (4)
191	350	(I_0+4)	→	(I_0+2)	25 (4)
198	1048	(I_0+9)	→	(I_0+8)	21 (4)
211	462	(I_0+5)	→	(I_0+3)	31 (10)
234	584	(I_0+6)	→	(I_0+4)	21 (6)
248	710	(I_0+7)	→	(I_0+5)	23 (6)
266	850	(I_0+8)	→	(I_0+6)	40 (6)
338	1048	(I_0+9)	→	(I_0+7)	38 (10)
356	1206	(I_0+10)	→	(I_0+8)	31 (10)
^{154}Pm					
94	94	(I_0+1)	→	(I_0)	43 (11)
109	203	(I_0+2)	→	(I_0+1)	43 (6)
126	329	(I_0+3)	→	(I_0+2)	46 (9)
141	470	(I_0+4)	→	(I_0+3)	71 (6)
158	628	(I_0+5)	→	(I_0+4)	20 (6)
174	802	(I_0+6)	→	(I_0+5)	29 (11)
189	991	(I_0+7)	→	(I_0+6)	17 (6)
203	203	(I_0+2)	→	(I_0)	40 (6)
235	329	(I_0+3)	→	(I_0+1)	100 (11)
267	470	(I_0+4)	→	(I_0+2)	83 (9)
299	628	(I_0+5)	→	(I_0+3)	97 (9)
331	802	(I_0+6)	→	(I_0+4)	69 (9)
363	991	(I_0+7)	→	(I_0+5)	63 (9)
397	1199	(I_0+8)	→	(I_0+6)	57 (9)
425	1416	(I_0+9)	→	(I_0+7)	69 (9)
464	1663	(I_0+10)	→	(I_0+8)	51 (11)
483	1899	(I_0+11)	→	(I_0+9)	74 (11)
^{156}Pm					
90	90	(I_0+1)	→	(I_0)	7 (3)
103	370	(I_0+4)	→	(I_0+3)	9 (3)
108	198	(I_0+2)	→	(I_0+1)	10 (1)
119	489	(I_0+5)	→	(I_0+4)	6 (1)
135	624	(I_0+6)	→	(I_0+5)	4 (1)
151	775	(I_0+7)	→	(I_0+6)	-[d]
172	370	(I_0+4)	→	(I_0+2)	10 (1)
198	198	(I_0+2)	→	(I_0)	6 (1)
222	489	(I_0+5)	→	(I_0+3)	7 (1)
236	326	(I_0+3)	→	(I_0+1)	6 (1)
254	624	(I_0+6)	→	(I_0+4)	9 (1)
271	469	(I_0+4)	→	(I_0+2)	9 (3)
286	775	(I_0+7)	→	(I_0+5)	9 (1)
307	633	(I_0+5)	→	(I_0+3)	7 (1)
319	943	(I_0+8)	→	(I_0+6)	10 (1)

TABLE II. *(Continued.)*

E_γ (keV)[a] ^{152}Pm	E_i (keV)[b]	J_i^π	→	J_f^π	I_γ[c](Err.)
341	810	(I_0+6)	→	(I_0+4)	6 (1)
350	1125	(I_0+9)	→	(I_0+7)	10 (4)
376	1009	(I_0+7)	→	(I_0+5)	6 (1)
384	1327	(I_0+10)	→	(I_0+8)	7 (1)
414	1539	(I_0+11)	→	(I_0+9)	10 (4)
443	1452	(I_0+9)	→	(I_0+7)	3 (1)
451	1778	(I_0+12)	→	(I_0+10)	6 (1)
475	2014	(I_0+13)	→	(I_0+11)	9 (1)

[a]γ-ray energy uncertainties are typically $\pm$ 0.2 keV, $\pm$ 0.5 keV and $\pm$ 1 keV around 200 keV, 500 keV, and 1 MeV, respectively.
[b]Level energies are given with respect to a level of energy x keV. The maximum uncertainty of the level energy is up to 0.5%.
[c]Intensities are normalized to 100 for ^{152,154}Pm and to 10 for ^{156}Pm. The errors quoted are the fitting errors.
[d]Weak transition, intensity could not be determined.

Strong β decay feeding to the ground state (1^+) and other low spin states (mostly 1^+) of ^{152}Pm are reported. The presence of two long-lived isomers with half-lives 7.5 min and $\approx$ 18 min were identified in ^{152}Pm and the most probable spin parity for these isomeric states were proposed to be of $4^\pm$ and $\geqslant 6^+$, respectively, based on the decay feeding to ^{152}Sm levels [18]. Though the total β-decay energy of the 7.5 min isomer was found to be 3.6 $\pm$ 0.1 MeV, the excitation energy of the proposed $\approx$ 18 min isomer could not be established. In the present work the prompt γ-ray spectrum obtained in coincidence with ^{152}Pm fragments is shown in Fig. 11(a). The information about the coincidence relationships of these γ rays has been obtained from the limited statistics of γ-γ coincidence from ^{238}U + ^{9}Be reaction. The coincidence spectrum corresponding to the sum of gates of 112 and 140 keV γ rays is shown in Fig. 12. The presence of 92-99-112-140-158-198 keV cascade can be seen from this spectrum. The (A, Z) gated γ rays of ^{152}Pm [Fig. 11(a)] are then used to obtain the coincidence information from the high-fold γ-γ-γ 3D cube and γ-γ-γ-γ 4D cubes from the Gammasphere data. A representative spectrum corresponding to the triple gate of 92-99-112 keV cascade is shown in Fig. 13. The level scheme, as shown in Fig. 14, is obtained from the γ-γ coincidence

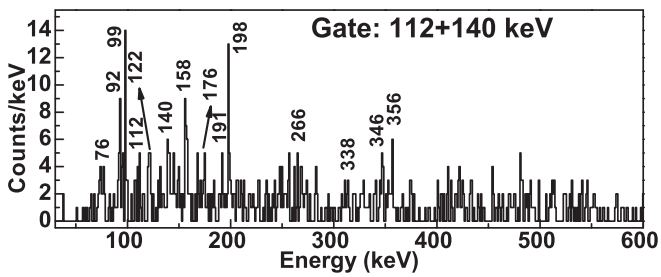

FIG. 12. Coincidence spectrum corresponding to the added gates of 112 and 140 keV transitions of ^{152}Pm, obtained from ^{238}U + ^{9}Be-induced fission data.

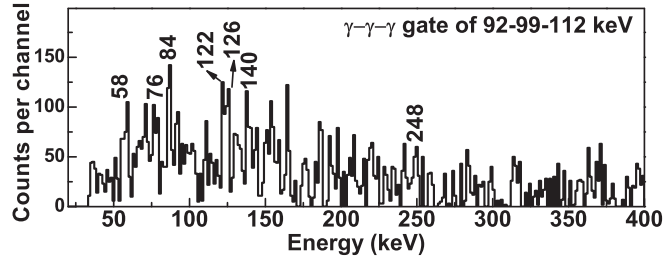

FIG. 13. Coincidence spectrum corresponding to triple gates of 92, 99, and 112 keV transitions of ^{152}Pm, obtained from ^{252}Cf fission.

information and the energy-sum systematics. As none of the γ rays, reported earlier from the β decay of ^{152}Nd [19], are observed in the present work, the excitation energy of the lowest level of ^{152}Pm from the current work cannot be established. As mentioned earlier, mainly high spin states are populated in fission reactions. As a result, the excited states of ^{152}Pm populated in the present work most probably decay to either of the known high spin isomeric states. Thus, the excitation energy and spin of the lowest level of the proposed scheme as $(0 + x)$ and I_0, respectively.

For ^{154}Pm, the γ-ray spectrum in coincidence with ^{154}Pm fragments detected from ^{238}U + ^{9}Be reaction, is shown in Fig. 11(b). The coincidence spectrum corresponding to some of the gates of 109, 126, and 141 keV γ rays are shown in Fig. 15. The spectra corresponding to the triple gates obtained from the high-fold γ coincidence data on spontaneous fission of ^{252}Cf at Gammasphere are shown in Fig. 16. The level scheme of ^{154}Pm proposed in the present work is shown in Fig. 17. It can be seen from the γ spectrum of Fig. 11(b) that several γ rays, such as, 99, 115, 133, 165, 179, 214, 248, 311, 344 keV, identified as belonging to ^{154}Pm, are not placed in the proposed level scheme. It is possible that these unassigned γ rays belong to a different band in ^{154}Pm. Though the excitation energy of the 2.68 min isomer (3, 4) is not known experimentally, this state is considered as the probable ground state from the consideration of β transition rates and expected two quasiparticle configuration [43] compared to the other 1.73 min isomer of proposed spin $(0^-, 1^-)$. Thus, in the

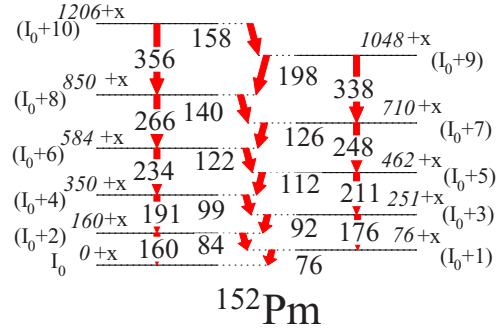

FIG. 14. Level scheme of ^{152}Pm proposed in the present work. All the new transitions in the scheme are from the present work and are shown in red. The level energies and tentative spin assignments are shown with respect to a level of energy $(0 + x)$ and spin I_0.

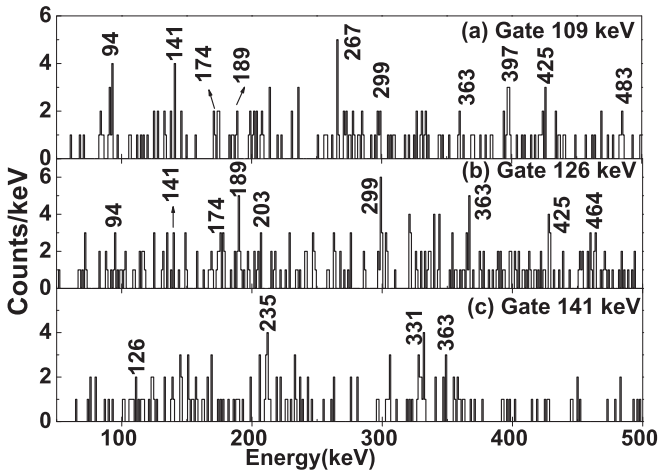

FIG. 15. Coincidence spectra corresponding to (a) 109, (b) 126, and (c) 141 keV gates of ^{154}Pm, obtained from ^{238}U + ^{9}Be-induced fission data.

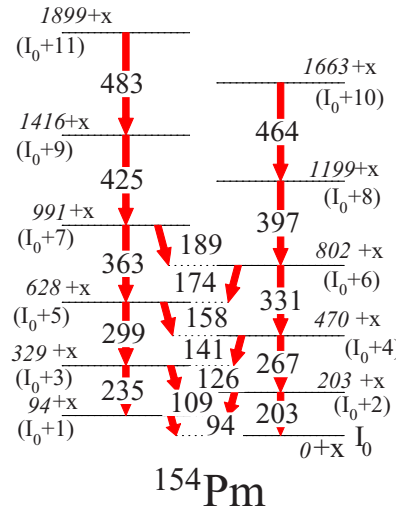

FIG. 17. Level scheme of ^{154}Pm proposed in the present work. All the new transitions in the scheme are from the present work and are shown in red. The level energies and tentative spin assignments are shown with respect to a level of energy $(0 + x)$ and spin I_0.

case of ^{154}Pm, the proposed level scheme can most probably be built on the 2.68 min (3, 4) state. But, as the energy of the 2.68 min (3, 4) state is not established experimentally, the lowest level of the proposed scheme of Fig. 17 is marked as $(0 + x)$, I_0.

The γ-ray spectrum of ^{156}Pm obtained in the present work from ^{238}U + ^{9}Be reaction, in coincidence with ^{156}Pm fragments identified in the focal plane of VAMOS++ spectrometer is shown in Fig. 11(c). It may be noted that none of the γ rays assigned to ^{156}Pm, from the previous study of spontaneous fission of ^{252}Cf by Hwang *et al.* [26], could be observed in this spectrum. These γ rays are now assigned to ^{157}Pm in the present work, as described in Sec. III A. Thus the unique identification of γ rays in case of such an exotic nucleus was difficult from ^{252}Cf spontaneous fission measurements, where the high-fold γ coincidences and the cross coincidence relationship among the fission fragment partners are utilized to assign the γ rays to a particular nucleus. In

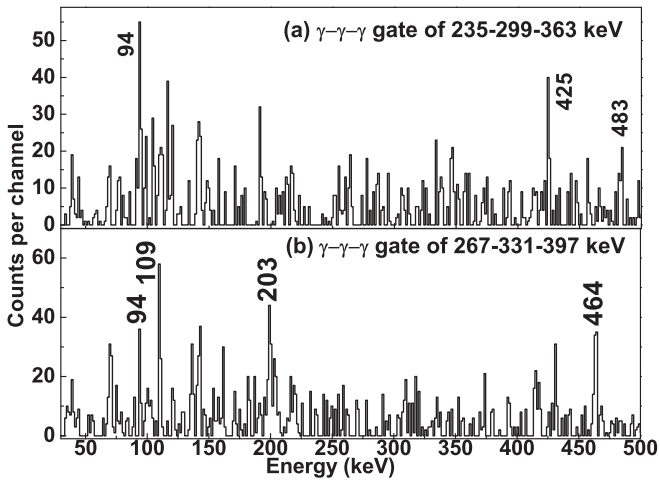

FIG. 16. Coincidence spectra corresponding to triple gates of (a) 235-299-363 keV and (b) 267-331-397 keV transitions of ^{154}Pm, obtained from ^{252}Cf fission.

the present work, as the fragments are directly identified at the focal plane of the spectrometer by (A, Z) tagging, the corresponding coincident γ rays are uniquely assigned to that particular fragment. Within the limited statistics of (A, Z) gated data from ^{238}U + ^{9}Be reaction, no γ-γ coincidence information could be obtained. However, the coincidence relationship among various γ rays identified in the (A, Z) gated spectrum could be obtained from the high-fold data from the spontaneous fission of ^{252}Cf, measured using the Gammasphere array. The coincidence spectra corresponding to the triple gates of γ transitions of ^{156}Pm are shown in Fig. 18. It may be noted that in these coincidence spectra from ^{252}Cf fission data, the γ rays of the corresponding fission partner can also be present in coincidence, as there is no (A, Z) selection in this case. The 142 keV strong transition observed in each coincidence spectra of Fig. 18, is actually from the fission partner ^{92}Rb. The level scheme, shown in Fig. 19, is obtained from the coincidence relationship among various γ-ray cascades. The low-energy transition of 68 keV is tentatively placed, as the transitions placed above and below the 68 keV are found to be in coincidence. Shibata *et al.* [23] earlier reported γ rays from the β decay of ^{156}Nd and did not propose any level scheme, except for the isomeric transition decay. It is possible that the present level scheme of ^{156}Pm is built on the ground state, which is proposed to be of higher spin $(J = 4)$ compared to the known isomeric state at 150.3 keV. A ground state of $4^{(-)}$ was proposed in Ref. [23], with the observation of a $M3$ transition from the (1^-) isomer. However, in Ref. [44], the most probable ground state is adopted to be a $4^{(+)}$ and the isomer as (1^+). From the discussion of Refs. [23,44], it appears that configurations corresponding to both $4^{(+)}$ and $4^{(-)}$ can be present in this region. Though some of the γ rays reported in Ref. [23] are found to have energies close to those assigned to ^{156}Pm in the present work, it cannot be firmly concluded that the

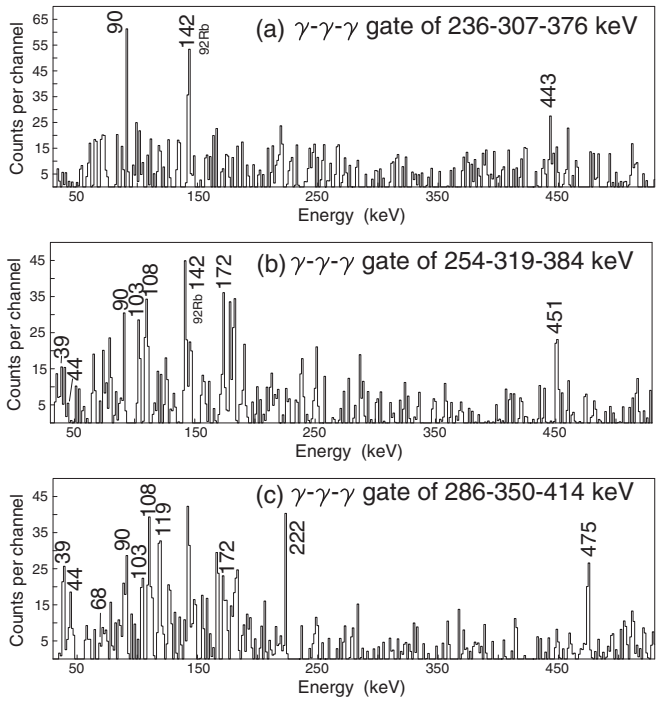

FIG. 18. Coincidence spectra corresponding to triple gates of (a) 236-307-376 keV, (b) 254-319-384 keV, and (c) 286-350-414 keV transitions of ^{156}Pm, obtained from ^{252}Cf fission.

corresponding excited states populated from β decay of ^{156}Nd are the same as that observed from the present work. Thus the possibility of placing the present level scheme to a state above the ground state cannot be ruled out. In view of above possibilities, we prefer to keep the lowest state of the proposed scheme as $(0+x, I_0)$.

The γ rays from the excited states of ^{158}Pm are identified for the first time in the present work and the corresponding spectrum is shown in Fig. 11(d). Seven new γ rays have been identified as belonging to ^{158}Pm from data of ^{238}U + ^{9}Be reaction. However, for ^{158}Pm, no level scheme could be obtained, as the statistics is very limited.

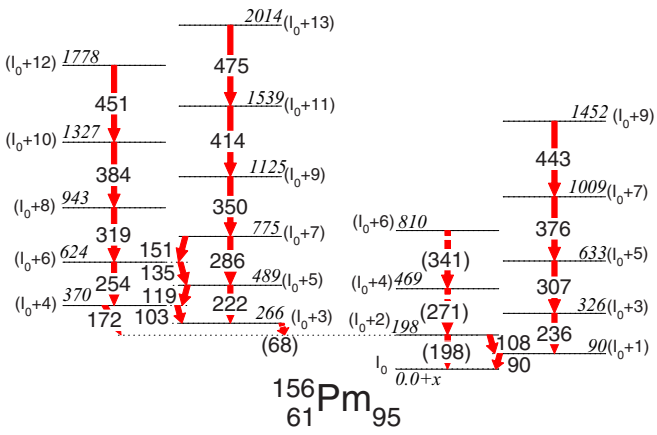

FIG. 19. Level scheme of ^{156}Pm proposed in the present work. All the new transitions in the scheme are from the present work and are shown in red. The level energies and tentative spin assignments are shown with respect to a level of energy $(0+x)$ and spin I_0.

IV. DISCUSSION

The nuclei under study are located at the boundary of octupole deformed lanthanide region (see Refs. [3,45]). If located in the vicinity of the respective Fermi levels, the deformed orbitals emerging from the proton $d_{5/2}$ and $h_{11/2}$ spherical subshells and from neutron $f_{7/2}$ and $i_{13/2}$ spherical subshells are responsible for possible occurrence of reflection asymmetric shapes. These spherical subshells satisfy the $\Delta j = \Delta l = 3$ condition, which leads to an increase of octupole correlations. The predictions of model calculations for the position of this boundary depend on the underlying mean field and its parametrization (see discussion in Sec. IV of Ref. [45]). For example, the highest neutron number for which covariant density functional calculations predict octupole deformation in the ground states of even-even Nd ($Z = 60$) nuclei is $N = 90$ for most of covariant energy density functionals. On the contrary, microscopic+macroscopic calculations and Hartree-Fock calculations with finite-range Gogny D1S force place this number at $N = 88$. Octupole deformation is even less pronounced in even-even Sm ($Z = 62$) nuclei; most model calculations place the boundary of the region of octupole deformation at $N = 88$ [45]. Note that even these nuclei are very soft in octupole deformation with very little gain in binding due to octupole deformation. Thus they are transitional in nature and octupole dynamical correlations (vibrations) are expected to play an important role in their structure.

However, the situation becomes more complicated in odd and odd-odd nuclei. There are two factors that can stabilize the octupole deformation in odd and odd-odd nucleus even if its even-even core does not have static octupole deformation. These are polarization effects of unpaired particles in specific Nilsson orbitals [12] and rotation [15]. Indeed, the 5/2[413] and 5/2[523] orbitals, located in the vicinity of the proton Fermi level of the Pm isotopes of interest, couple strongly through the Y_{30} operator [15]. However, polarization energies towards octupole deformation are weak for these orbitals for neutron numbers $N \geqslant 90$. So, neutron-rich Pm isotopes are not expected to show static octupole deformation at low spin. On the other hand, the static octupole deformation can be stabilized by rotation even if the nucleus is only octupole soft at spin zero [15]. Experimental data on parity doublet bands in ^{151}Pm and ^{153}Eu formed by the 5/2[523] and 5/2[413] rotational structures show all features of the approach of static octupole deformation at highest observed spins [16].

In ^{151}Pm, the opposite parity states of these two rotational sequences are connected by $E1$ transitions, which was interpreted as due to the presence of static octupole deformation [30]. The ground-state band in ^{151}Pm is a positive-parity $K = 5/2^+$ rotational band based on a 5/2[413] Nilsson orbital originating from $\pi g_{7/2}$. The negative parity band built on a $K = 5/2^-$ at an excitation energy of 117 keV is based on a $5/2^-$[532] Nilsson configuration originating from $\pi h_{11/2}$ orbital.

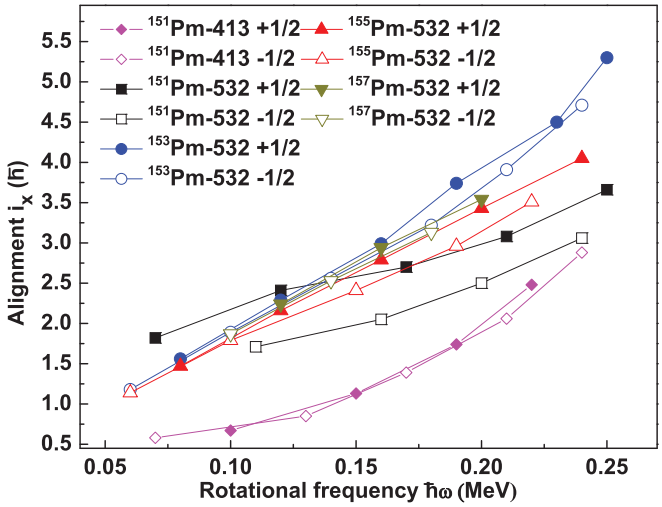

FIG. 20. Alignment plot for bands of all odd-A Pm isotopes from $N = 90$ to $N = 96$, produced in the present work. The different bands are marked by possible Nilsson configurations and corresponding signatures (α).

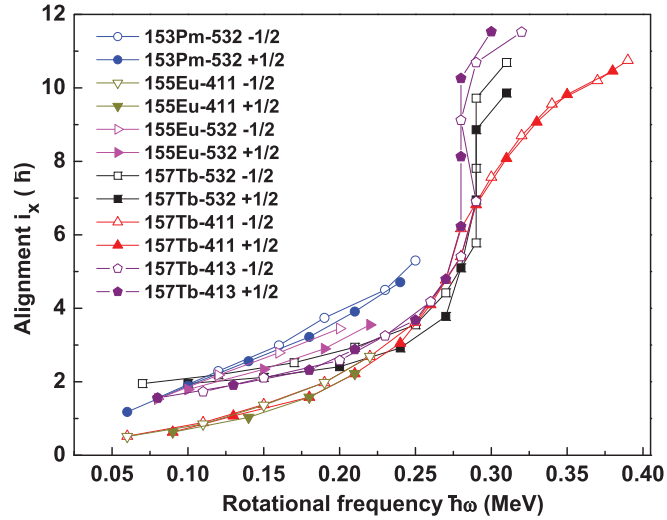

FIG. 21. Alignment plot for bands of all odd-A Pm isotopes from $N = 90$ to $N = 96$, produced in the present work. The possible configurations of the bands are as mentioned.

In case of ^{153}Pm, the yrast ground-state band built on $K = 5/2^-$ is known to be constituted from $5/2^-[532]$ Nilsson orbital [24], which originates from the deformation driving $\pi h_{11/2}$ orbital. In case of ^{151}Pm, this is the non-yrast structure and the yrast ground band is $5/2^+$ based on $5/2^+[413]$ configuration. Indeed, in the framework of rotation-vibration model, the level structure of ^{153}Pm, populated by β decay, is described as that of a deformed nucleus [20]. The single proton hole strength in ^{153}Pm was found to be largely fragmented from the study of transfer reactions [25]. In the present work, the excited band based on a $5/2^+[413]$ configuration in ^{153}Pm could not be extended to higher spin and is weakly populated. It is probably due to the fact that the deformation (quadrupole) driving effect of the $\pi h_{11/2}$ orbital makes ^{153}Pm to have larger prolate deformation compared to ^{151}Pm.

To understand the band structure in all odd-A Pm isotopes produced in the present work, the alignments [46] of both favored and unfavored signature partner bands are plotted in Fig. 20 as a function of rotational frequency. The Harris parameters [47] with $J_0 = 34.3\ \hbar^2/\text{MeV}$ and $J_1 = 45.0\ \hbar^4/\text{MeV}^3$ have been used to subtract the contributions of core angular momentum, which is considered as ^{156}Gd in this case. From the alignment plot of Fig. 20, it is evident that the slopes of the alignments for the bands in ^{151}Pm ($N = 90$) are significantly different compared to all other odd-A Pm isotopes with higher N/Z. This is due to the fact that the nature of the bands in ^{151}Pm is different as compared to corresponding bands in odd-A Pm isotopes with higher N. The higher alignment at higher frequency in case of odd-A Pm isotopes $^{153-157}$Pm compared to ^{151}Pm is evident as due to the involvement of high-$j h_{11/2}$ orbital. The alignments of the bands in $^{155-157}$Pm are quite similar to that of the ground band in ^{153}Pm, which is based on the 5/2[532] configuration originating from the $h_{11/2}$ orbital. This suggests the same 5/2[532] configuration assignment to the observed negative parity bands in ^{155,157}Pm. In Fig. 21 the alignments of the $K = 5/2^+$ and $K = 5/2^-$ bands in ^{153}Pm are compared with the bands having same configurations and with other configurations in neighboring $N = 92$ isotones of ^{157}Tb and ^{155}Eu. In case of ^{157}Tb, the $3/2^+[411]$ band was found to be the ground-state band [14], whereas in ^{155}Eu the $5/2^+[413]$ band becomes the ground-state band. The $5/2^-[532]$ band, which is the ground band in ^{153}Pm was also observed in both ^{155}Eu and ^{157}Tb. For the 5/2[532] band in ^{157}Tb, the back-bending occurs at the frequency $\hbar\omega \sim 0.28$ MeV due to the alignment of two $i_{13/2}$ neutrons. It can be seen that the same band in ^{153}Pm could be observed in the present work up to the frequency corresponding to the up-bend of the alignment.

The energy staggerings of the states in rotational bands of odd-A $^{151-157}$ isotopes are shown in Fig. 22 as a function of spin. From the observed signature splitting it is evident

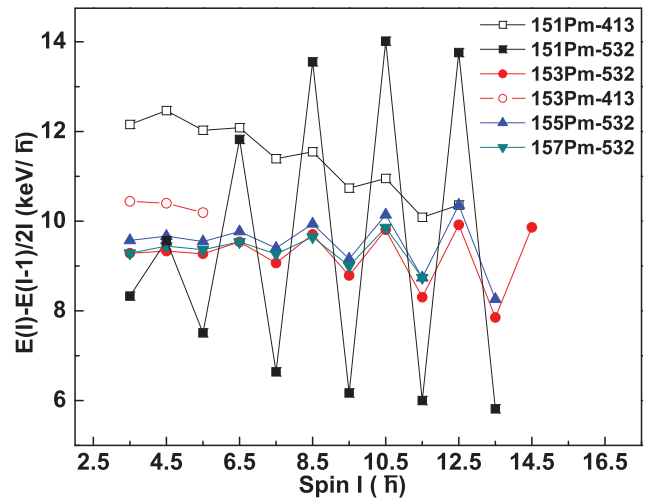

FIG. 22. Energy staggering as a function of spin for the bands of all odd-A Pm isotopes from $N = 90$ to $N = 96$, produced in the present work.

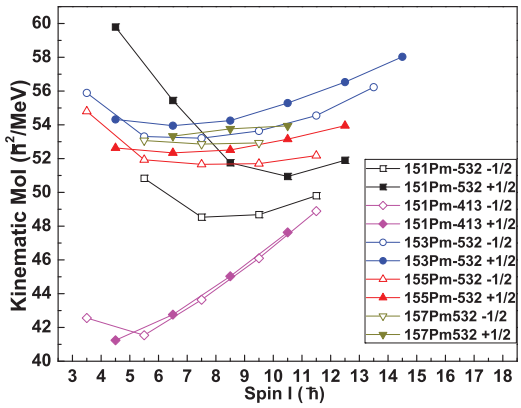

FIG. 23. Kinematic moment of inertia (MoI) as a function of spin of the bands of all odd-A Pm isotopes from $N = 90$ to $N = 96$, produced in the present work.

that the negative parity band in ^{151}Pm, corresponding to the $5/2^-[532]$ orbital shows pronounced splitting compared to the positive parity band corresponding to the $5/2^+[413]$ Nilsson orbital. The odd-A Pm isotopes with higher N/Z show modest signature splitting at higher spins. The kinematic moment of inertia (J_1) of the bands in odd-A Pm isotopes for both favored and unfavored signature partners are plotted in Fig. 23. The moments of inertia of $5/2^-[532]$ bands in ^{153,155,157}Pm isotopes increase at higher spins.

In order to better understand the experimental features of the observed bands, proton quasiparticle Routhian diagrams for even-even nuclei neighboring to ^{155}Pm are shown in Fig. 24. They have been obtained in the cranked relativistic Hartree-Bogoliubov calculations (Ref. [48]) employing two covariant energy density functionals (CEDFs), namely, NL1 [49] and NL3* [50]. Although the calculated quasiparticle energies somewhat depend on the employed functional, the rotational features of the Routhians of interest are independent on its choice. For example, in all panels of Fig. 24 the lowest positive parity Routhians are based on the 5/2[413] orbital. These Routhians are signature degenerated, which is similar

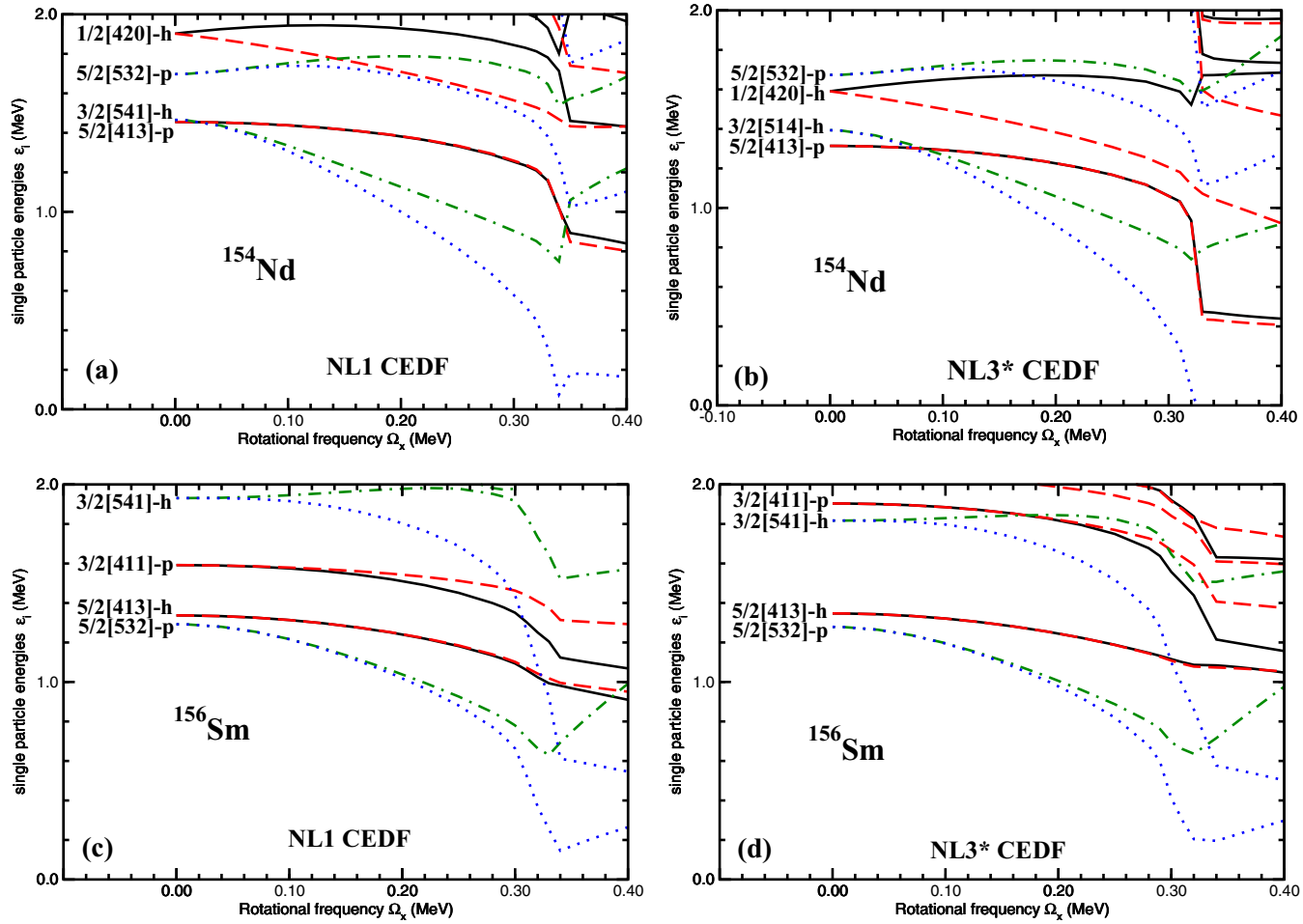

FIG. 24. Proton quasiparticle energies corresponding to the lowest configurations in the indicated nuclei. They are given along the deformation path of these configurations. The CRHB+LN calculations have been performed with the NL1 (left panels) and NL3* (right panels) CEDFs. Long-dashed, solid, dot-dashed, and dotted lines indicate $(\pi = +, r = +i)$, $(\pi = +, r = -i)$, $(\pi = -, r = +i)$, and $(\pi = -, r = -i)$ orbitals, respectively. At $\Omega_x = 0.0$ MeV, the quasiparticle orbitals are labeled by the asymptotic quantum numbers $[Nn_z\Lambda]\Omega$ (Nilsson quantum numbers) of the dominant component of the wave function. The letters "p" and "h" before the Nilsson labels are used to indicate whether a given Routhian is of particle ($V^2 < 0.5$) or hole ($V^2 > 0.5$) type.

to the properties of the experimental 5/2[413] bands seen in ^{151,153}Pm nuclei. The lowest two calculated pairs of negative parity Routhians are based on the 5/2[532] and 3/2[514] orbitals and their rotational properties depend on the position of the proton Fermi surface. This surface is more bound in the $Z = 60$ Nd nuclei. As a consequence, the 3/2[514] Routhians are the lowest in energy. The interaction of hole-type 3/2[514] and particle-type 5/2[532] orbitals leads to substantial signature splitting in both orbitals. However, with increasing the energy of the Fermi surface on going to the $Z = 62$ Sm isotopes the 5/2[532] orbital becomes the lowest in energy negative parity orbital and the coupling between the above-mentioned negative parity orbitals is significantly reduced. As a consequence, the 5/2[532] orbital is signature degenerated at very low frequencies but small signature degeneracy gradually develops with increasing rotational frequency. This feature is very similar to what is seen in experimental 5/2[532] bands of ^{153,155,157}Pm (see Figs. 21, 22, and 23). In addition to the possible role of static octupole deformation in the structure of the 5/2[532] and 5/2[413] bands of ^{151}Pm discussed in Ref. [16], it is quite likely that large signature splitting seen in the 5/2[532] band of this nuclei is the consequence of the interaction of the 5/2[532] and 5/2[413] orbitals (seen in the top panels of Fig. 24), which has been discussed above.

For the odd-odd Pm isotopes, the low-lying high-spin isomers are interpreted in the framework of quasiparticle-rotor model as two-quasiparticle structures [43,51]. The proposed band structures in the present work can either be built just above the isomeric state, or above another excited state, which may exist very close to the isomeric level. Due to the lack of firm spin and parity assignment to the band structure built above the long-lived isomers, reasonable configuration assignments to the observed bands cannot be made.

V. SUMMARY AND CONCLUSIONS

In summary the neutron-rich $^{152-158}$Pm isotopes have been characterized using in-beam prompt γ-ray spectroscopy of isotopically identified fission fragments and high-fold coincidence data of ^{252}Cf spontaneous fission. New results of odd-odd Pm isotopes above the long-lived isomeric states have been reported for the first time. The rotational band structures of odd-A Pm isotopes with neutron numbers up to $N = 96$ have been extended to higher spins. The configuration assignment to the rotational structures in odd-A isotopes are understood from the systematics of band properties and in terms of Routhians of the neighboring even-even isotopes, obtained from cranked relativistic Hartree-Bogoliubov calculations. The observed band structures of odd-A Pm isotopes do not show any indication of presence of octupole deformation beyond $N = 90$.

ACKNOWLEDGMENTS

We would like to thank J. Goupil, G. Fremont, L. Ménager, J. Ropert, C. Spitaels, and the GANIL accelerator staff for their technical contributions and C. Schmitt for help in various aspects of data collection, analysis, and many useful discussions. The authors would also like to thank the anonymous referee for a very critical reading of the manuscript and for useful suggestions in improving the clarity of the manuscript. Two of us (S.B. and S.B.) acknowledge partial financial support through the LIA France-India agreement. The support of CEFIPRA/IFCPAR under Project No. 5604-4 is also acknowledged. The work at Vanderbilt University and Lawrence Berkeley National Laboratory is supported by the U.S. Department of Energy under Grant No. DE-FG05-88ER40407 and Contract No. DE-AC03-76SF00098. The work at Tsinghua University was supported by the National Natural Science Foundation of China under Grant No. 11175095. The work at JINR was partially supported by the Russian Foundation for Basic Research Grant No. 08-02-00089 and by the INTAS Grant No. 03-51-4496. This material is based upon work supported by the U.S. Department of Energy, Office of Science, Office of Nuclear Physics under Award No. DE-SC0013037 (Mississippi State University).

[1] R. F. Casten, D. D. Warner, D. S. Brenner, and R. L. Gill, Phys. Rev. Lett. **47**, 1433 (1981).
[2] I. Ahmad and P. A. Butler, Annu. Rev. Nucl. Part. Sci. **43**, 71 (1993).
[3] P. A. Butler and W. Nazarewicz, Rev. Mod. Phys. **68**, 349 (1996).
[4] G. A. Leander, W. Nazarewicz, P. Olanders, I. Ragnarsson, and J. Dudek, Phys. Lett. B **152**, 284 (1985).
[5] W. R. Phillips, I. Ahmad, H. Emling, R. Holzmann, R. V. F. Janssens, T.-L. Khoo, and M. W. Drigert, Phys. Rev. Lett. **57**, 3257 (1986).
[6] S. J. Zhu *et al.*, Phys. Lett. B **357**, 273 (1995).
[7] S. J. Zhu, J. H. Hamilton, A. V. Ramayya, E. F. Jones, J. K. Hwang, M. G. Wang, X. Q. Zhang, P. M. Gore, L. K. Peker, G. Drafta, B. R. S. Babu, W. C. Ma, G. L. Long, L. Y. Zhu, C. Y. Gan, L. M. Yang, M. Sakhaee, M. Li, J. K. Deng, T. N. Ginter, C. J. Beyer, J. Kormicki, J. D. Cole, R. Aryaeinejad, M. W. Drigert, J. O. Rasmussen, S. Asztalos, I. Y. Lee, A. O. Macchiavelli, S. Y. Chu, K. E. Gregorich, M. F. Mohar, G. M. Ter-Akopian, A. V. Daniel, Y. T. Oganessian, R. Donangelo, M. A. Stoyer, R. W. Lougheed, K. J. Moody, J. F. Wild, S. G. Prussin, J. Kliman, and H. C. Griffin, Phys. Rev. C **60**, 051304(R) (1999).
[8] Y. J. Chen *et al.*, Phys. Rev. C **73**, 054316 (2006).
[9] N. T. Brewer, Ph.D. thesis, Vanderbilt University, Nashvillle, TN, 2013.
[10] R. K. Sheline and P. C. Sood, Phys. Rev. C **34**, 2362 (1986).
[11] B. Bucher, S. Zhu, C. Y. Wu, R. V. F. Janssens, D. Cline, A. B. Hayes, M. Albers, A. D. Ayangeakaa, P. A. Butler, C. M. Campbell, M. P. Carpenter, C. J. Chiara, J. A. Clark, H. L. Crawford, M. Cromaz, H. M. David, C. Dickerson, E. T. Gregor, J. Harker, C. R. Hoffman, B. P. Kay, F. G. Kondev, A. Korichi, T. Lauritsen, A. O. Macchiavelli, R. C. Pardo, A. Richard, M. A. Riley, G. Savard, M. Scheck, D. Seweryniak, M. K. Smith, R. Vondrasek, and A. Wiens, Phys. Rev. Lett. **116**, 112503 (2016).

[12] A. V. Afanasjev and I. Ragnarsson, Phys. Rev. C **51**, 1259 (1995).
[13] P. A. Butler and W. Nazarewicz, Nucl. Phys. A **533**, 249 (1991).
[14] D. J. Hartley, M. A. Riley, D. E. Archer, T. B. Brown, J. Döring, R. A. Kaye, F. G. Kondev, T. Petters, J. Pfohl, R. K. Sheline, S. L. Tabor, and J. Simpson, Phys. Rev. C **57**, 2944 (1998).
[15] W. Nazarewicz and S. L. Tabor, Phys. Rev. C **45**, 2226 (1992).
[16] A. V. Afanasjev, J. Phys. G: Nucl. Part. Phys **19**, L143 (1993).
[17] G. A. Leander and R. K. Sheline, Nucl. Phys. A **413**, 375 (1984).
[18] W. R. Daniels and D. C. Hoffman, Phys. Rev. C **4**, 919 (1971).
[19] M. Shibata, M. Asai, T. Ikuta, H. Yamamoto, J. Ruan, K. Okano, K. Aoki and K. Kawade *et al.*, Appl. Rad. Isot. **44**, 923 (1993).
[20] A. Taniguchi *et al.*, J. Phys. Soc. Jpn. **65**, 3824 (1996).
[21] T. Karlewski *et al.*, Z. Phys. A **322**, 177 (1985).
[22] R. C. Greenwood, R. A. Anderl, J. D. Cole, and H. Willmes, Phys. Rev. C **35**, 1965 (1987).
[23] M. Shibata *et al.*, Eur. Phys. J. A **31**, 171 (2007).
[24] D. G. Burke, G. Lovhoiden, E. R. Flynn, and J. W. Sunier, Phys. Rev. C **18**, 693 (1978).
[25] I. S. Lee *et al.*, Nucl. Phys. A **371**, 111 (1981).
[26] J. K. Hwang, A. V. Ramayya, J. H. Hamilton, S. H. Liu, K. Li, H. L. Crowell, C. Goodin, Y. X. Luo, J. O. Rasmussen, and S. J. Zhu, Phys. Rev. C **80**, 037304 (2009).
[27] W. Urban *et al.*, Nucl. Phys. A **587**, 541 (1995).
[28] M. A. Jones *et al.*, Nucl. Phys. A **609**, 201 (1996).
[29] W. J. Vermeer, M. K. Khan, A. S. Mowbray, J. B. Fitzgerald, J. A. Cizewski, B. J. Varley, J. L. Durell, and W. R. Phillips, Phys. Rev. C **42**, R1183 (1990).
[30] W. Urban *et al.*, Phys. Lett. B **247**, 238 (1990).
[31] R. Yokoyama *et al.*, JPS Conf. Proc. **6**, 030021 (2015).
[32] J. M. D'auria, D. Ostrom, and S. C. Gujrathi, Nucl. Phys. A **178**, 172 (1971).
[33] J. Simpson *et al.*, Acta Physica Hungarica, New Series, Heavy Ion Physics **11**, 159 (2000).
[34] M. Rejmund *et al.*, Nucl. Instr. Meth. A **646**, 184 (2011); S. Pullanhiotan *et al.*, *ibid.* **593**, 343 (2008).
[35] E. H. Wang, A. Lemasson, J. H. Hamilton, A. V. Ramayya, J. K. Hwang, J. M. Eldridge, A. Navin, M. Rejmund, S. Bhattacharyya, S. H. Liu, N. T. Brewer, Y. X. Luo, J. O. Rasmussen, H. L. Liu, H. Zhou, Y. X. Liu, H. J. Li, Y. Sun, F. R. Xu, S. J. Zhu, G. M. Ter-Akopian, Y. T. Oganessian, M. Caamano, E. Clement, O. Delaune, F. Farget, G. deFrance, and B. Jacquot, Phys. Rev. C **92**, 034317 (2015).
[36] S. Bhattacharyya, M. Rejmund, A. Navin, E. Caurier, F. Nowacki, A. Poves, R. Chapman, D. O'Donnell, M. Gelin, A. Hodsdon, X. Liang, W. Mittig, G. Mukherjee, F. Rejmund, M. Rousseau, P. Roussel-Chomaz, K.-M. Spohr, and C. Theisen, Phys. Rev. Lett. **101**, 032501 (2008).
[37] A. Navin and M. Rejmund, in *McGraw-Hill Yearbook of Science and Technology* (McGraw-Hill, New York, 2014), p. 137.
[38] A. Navin *et al.*, Phys. Lett. B **728**, 136 (2014).
[39] D. C. Radford, Nucl. Instrum. Meth. A **361**, 297 (1995).
[40] S. J. Zhu, M. Sakhaee, J. H. Hamilton, A. V. Ramayya, N. T. Brewer, J. K. Hwang, S. H. Liu, E. Y. Yeoh, Z. G. Xiao, Q. Xu, Z. Zhang, Y. X. Luo, J. O. Rasmussen, I. Y. Lee, K. Li, and W. C. Ma, Phys. Rev. C **85**, 014330 (2012).
[41] H. J. Li, S. J. Zhu, J. H. Hamilton, A. V. Ramayya, J. K. Hwang, Y. X. Liu, Y. Sun, Z. G. Xiao, E. H. Wang, J. M. Eldridge, Z. Zhang, Y. X. Luo, J. O. Rasmussen, I. Y. Lee, G. M. Ter-Akopian, A. V. Daniel, Y. T. Oganessian, and W. C. Ma, Phys. Rev. C **88**, 054311 (2013).
[42] R. C. Greenwood *et al.*, Nucl. Instrum. Meth. A **390**, 95 (1997).
[43] P. C. Sood and R. K. Sheline, Pramana **35**, 329 (1990).
[44] C. W. Reich, NDS **113**, 2537 (2012).
[45] S. E. Agbemava, A. V. Afanasjev, and P. Ring, Phys. Rev. C **93**, 044304 (2016).
[46] R. Bengtsson, S. Frauendorf, and F. R. May, At. Data Nucl. Data Tables **35**, 15 (1986).
[47] S. M. Haris, Phys. Rev. **138**, B509 (1965).
[48] A. V. Afanasjev, P. Ring, and J. König, Nucl. Phys. A **676**, 196 (2000).
[49] P.-G. Reinhard *et al.*, Z. Phys. A **323**, 13 (1986).
[50] G. A. Lalazissis *et al.*, Phys. Lett. B **671**, 36 (2009).
[51] P. C. Sood, M. Sainath, R. Gowrishankar, and K. V. Sai, Phys. Rev. C **83**, 027303 (2011).